

**Supplementary data for**

Novel magnetic composite adsorbent of phenolic compounds based on waste poly(ethylene terephthalate) and carbon encapsulated magnetic nanoparticles

P. Strachowski<sup>1</sup>, W. Kaszuwara<sup>2</sup> and M. Bystrzejewski<sup>1\*</sup>

<sup>1</sup>Faculty of Chemistry, University of Warsaw, Pasteur 1 str., 02-093 Warsaw, Poland

<sup>2</sup>Faculty of Materials Science, Warsaw University of Technology, 00-141 Warsaw, Poland

\*Email corresponding author: mibys@chem.uw.edu.pl

Table S1. Total yield, Fe content, saturation magnetization ( $M_s$ ), coercive field and G/D ratio of studied composites.

	Total yield (%)	Fe content (wt. %)	$M_s$ (emu/g)	Coercive field (Oe)	G/D
Activated carbon	-	-	-	-	0.60
Pure CEINs	-	47.4	64.0	330	2.44
PET(KOH)-9	11	5.71	10.4	273	0.45
PET(KOH)-23	21	18.6	27.4	309	0.38
PET(KOH)-44	26	33.1	54.3	352	0.62
PET(ZnCl <sub>2</sub> )-9	18	3.79	5.7	182	0.37
PET(ZnCl <sub>2</sub> )-23	25	6.81	11.1	276	0.27
PET(ZnCl <sub>2</sub> )-44	31	14.1	29.0	242	0.32
PET(CO <sub>2</sub> ) 550°C	15	8.96	14.5	254	0.55
PET(CO <sub>2</sub> ) 600°C	17	8.61	15.8	256	0.48
PET(CO <sub>2</sub> ) 700°C	7	10.1	14.6	311	1.23

Table S2. Langmuir adsorption isotherm parameters.

	Phenol			2-chlorophenol			4-chlorophenol		
	q <sub>max</sub> (mg/g)	K <sub>L</sub> (L/mg)	R <sup>2</sup>	q <sub>max</sub> (mg/g)	K <sub>L</sub> (L/mg)	R <sup>2</sup>	q <sub>max</sub> (mg/g)	K <sub>L</sub> (L/mg)	R <sup>2</sup>
AC commercial	283	0.008	0.999	549.5	0.011	0.999	280	0.142	0.999
PET(KOH)-9	124	0.072	0.999	204	0.032	0.975	269	0.016	0.986
PET(KOH)-23	69	0.046	0.998	99	0.063	0.985	107	0.032	0.995
PET(KOH)-44	15	0.045	0.975	37	0.060	0.993	45	0.093	0.999
PET(ZnCl <sub>2</sub> ) – 9	118	0.062	0.999	358	0.031	0.972	223	0.23	0.990
PET(ZnCl <sub>2</sub> ) – 23	67	0.161	0.998	128	0.176	0.996	126	0.427	0.999
PET(ZnCl <sub>2</sub> ) – 44	15	0.022	0.995	40	0.195	0.992	64	0.047	0.992
PET(CO <sub>2</sub> ) 600°C	29.1	0.176	0.990	90.1	0.047	0.978	87.8	0.035	0.995

Table S3. Mathematical formulas of kinetics theoretical models

Kinetic model	nonlinear form	Linear form	Plot
Pseudo-second order	$q_t = \frac{q_e t}{(1/k_2 q_e) + t}$	$\frac{t}{q_t} = \frac{1}{k_2 q_e^2} + \frac{1}{q_e} t$	$\frac{t}{q_t}$ vs. $t$
Intra-particle diffusion	-	$q_t = K_D t^{0.5} + \theta$	$q_t$ vs. $t^{0.5}$

Table S4. Adsorption kinetics rates of phenolic compounds onto studied materials.

	Phenol		2-chlorophenol		4-chlorophenol	
	$K_2$ (g/mg min)	$R^2$	$K_2$ (g/mg min)	$R^2$	$K_2$ (g/mg min)	$R^2$
AC commercial	$0,45 \cdot 10^{-3}$	0,999	$0,27 \cdot 10^{-3}$	0,995	$0,19 \cdot 10^{-3}$	0,998
PET(KOH)-9	$0,18 \cdot 10^{-3}$	0,997	$3,63 \cdot 10^{-3}$	0,999	$1,32 \cdot 10^{-3}$	0,999
PET(KOH)-23	$1,2 \cdot 10^{-3}$	0,999	$0,80 \cdot 10^{-3}$	0,999	$1,60 \cdot 10^{-3}$	0,998
PET(KOH)-44	$5,3 \cdot 10^{-3}$	0,998	$3,28 \cdot 10^{-3}$	0,999	$4,75 \cdot 10^{-3}$	0,995
PET(ZnCl <sub>2</sub> )-9	$0,52 \cdot 10^{-3}$	0,992	$8,17 \cdot 10^{-3}$	0,999	$0,55 \cdot 10^{-3}$	0,999
PET(ZnCl <sub>2</sub> )-23	$1,4 \cdot 10^{-3}$	0,998	$1,44 \cdot 10^{-3}$	0,998	$0,78 \cdot 10^{-3}$	0,997
PET(ZnCl <sub>2</sub> )-44	$5,8 \cdot 10^{-3}$	0,991	$4,95 \cdot 10^{-3}$	0,999	$1,63 \cdot 10^{-3}$	0,996
PET(CO <sub>2</sub> )-600	$1,55 \cdot 10^{-3}$	0,993	$1,48 \cdot 10^{-3}$	0,999	$0,0069 \cdot 10^{-3}$	0,919

Table S5. Intra-particle ( $K_D$ ) and film diffusion ( $\Theta$ ) rates for adsorption of phenolic compounds onto studied composites.

	Phenol		2-chlorophenol		4-chlorophenol	
	$K_D$ (g/mg s <sup>0.5</sup> )	$\Theta$ (mg/g)	$K_D$ (g/mg s <sup>0.5</sup> )	$\Theta$ (mg/g)	$K_D$ (g/mg s <sup>0.5</sup> )	$\Theta$ (mg/g)
AC commercial	28.76	8.59	14.27	28.56	28.58	-
PET(KOH)-9	4.77	22.46	1.36	101.44	4.31	19.80
PET(KOH)-23	9.03	4.17	2.25	50.11	3.71	18.43
PET(KOH)-44	1.09	1.97	4.21	-	3.11	2.58
PET(ZnCl <sub>2</sub> ) – 9	4.59	5.43	1.82	130.36	9.67	17.83
PET(ZnCl <sub>2</sub> ) – 23	1.13	31.72	7.41	7.92	7.43	36.12
PET(ZnCl <sub>2</sub> ) – 44	0.59	0.74	1.70	16.07	2.35	28.59
PET(CO <sub>2</sub> )-600	1.00	14.33	6.03	29.16	5.77	-

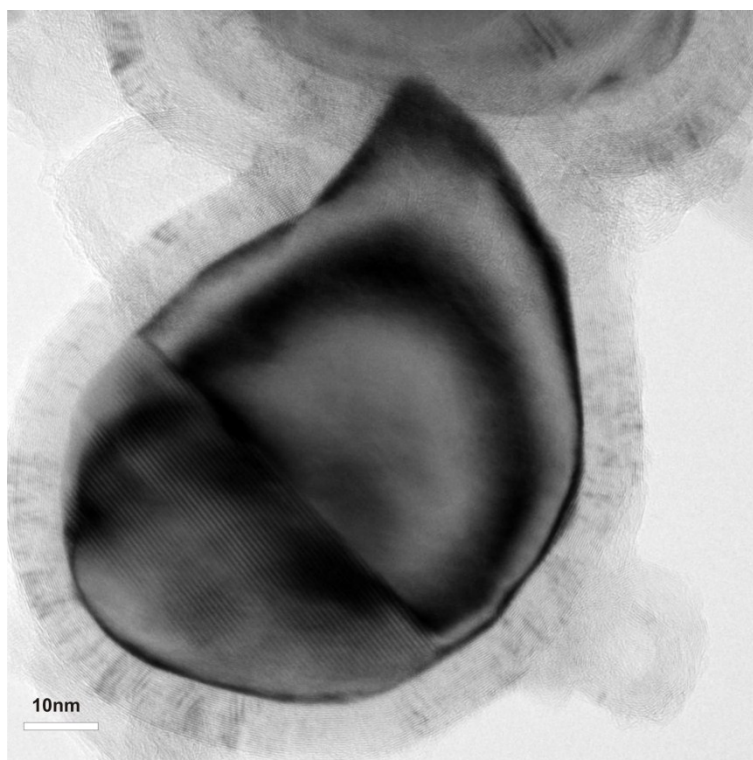


Figure S1. high-resolution TEM image of an individual CEIN particle.

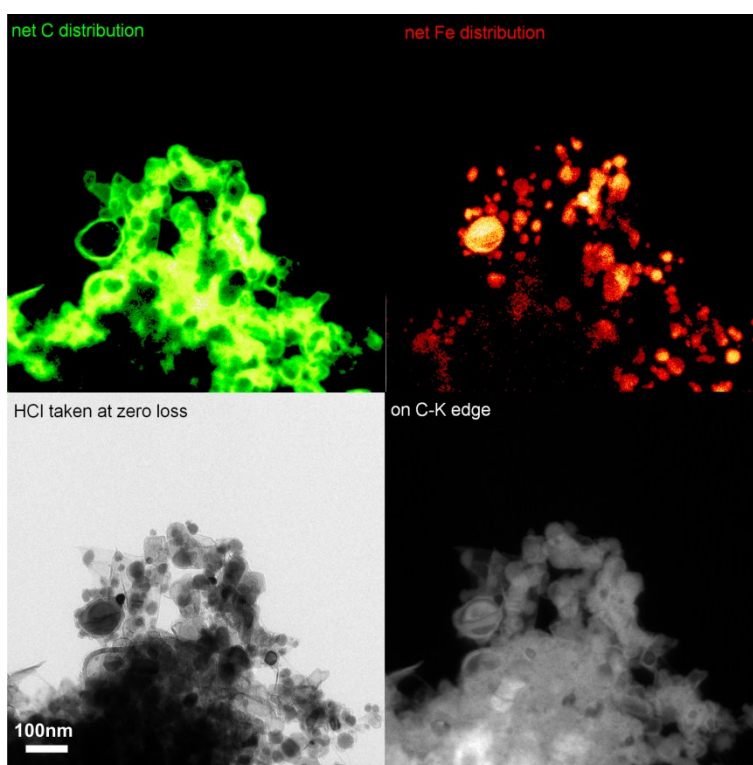


Figure S2. The distribution map of carbon and iron in CEINs structure.

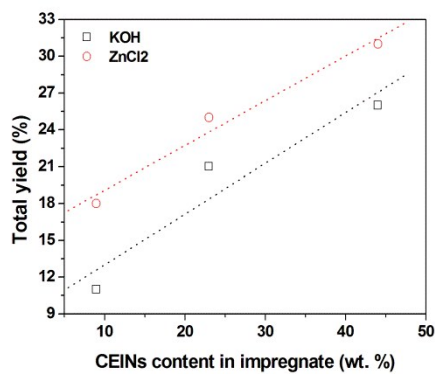


Figure S3. Total synthesis yield vs content of CEINs.

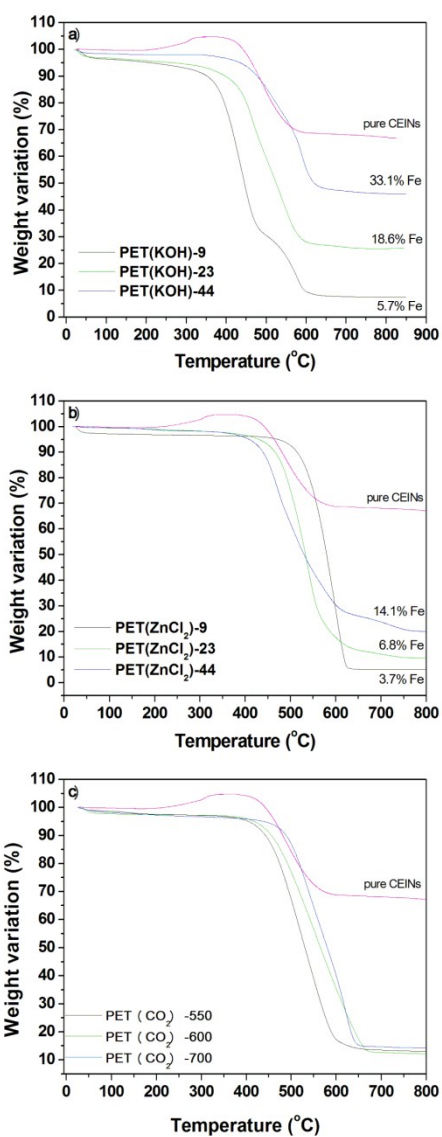


Figure S4. Thermogravimetric curves of (a) KOH activated composites, (b) ZnCl<sub>2</sub> activated composites, (c) CO<sub>2</sub> activated composites in comparison with pure CEINs.

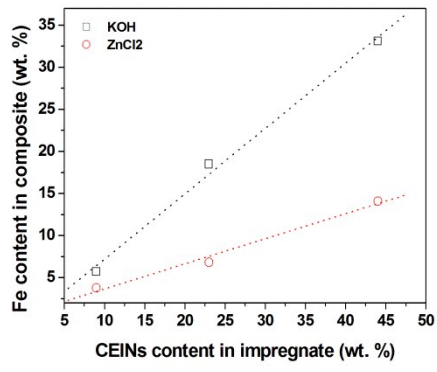


Figure S5. Fe content in composites vs. content of CEINs.

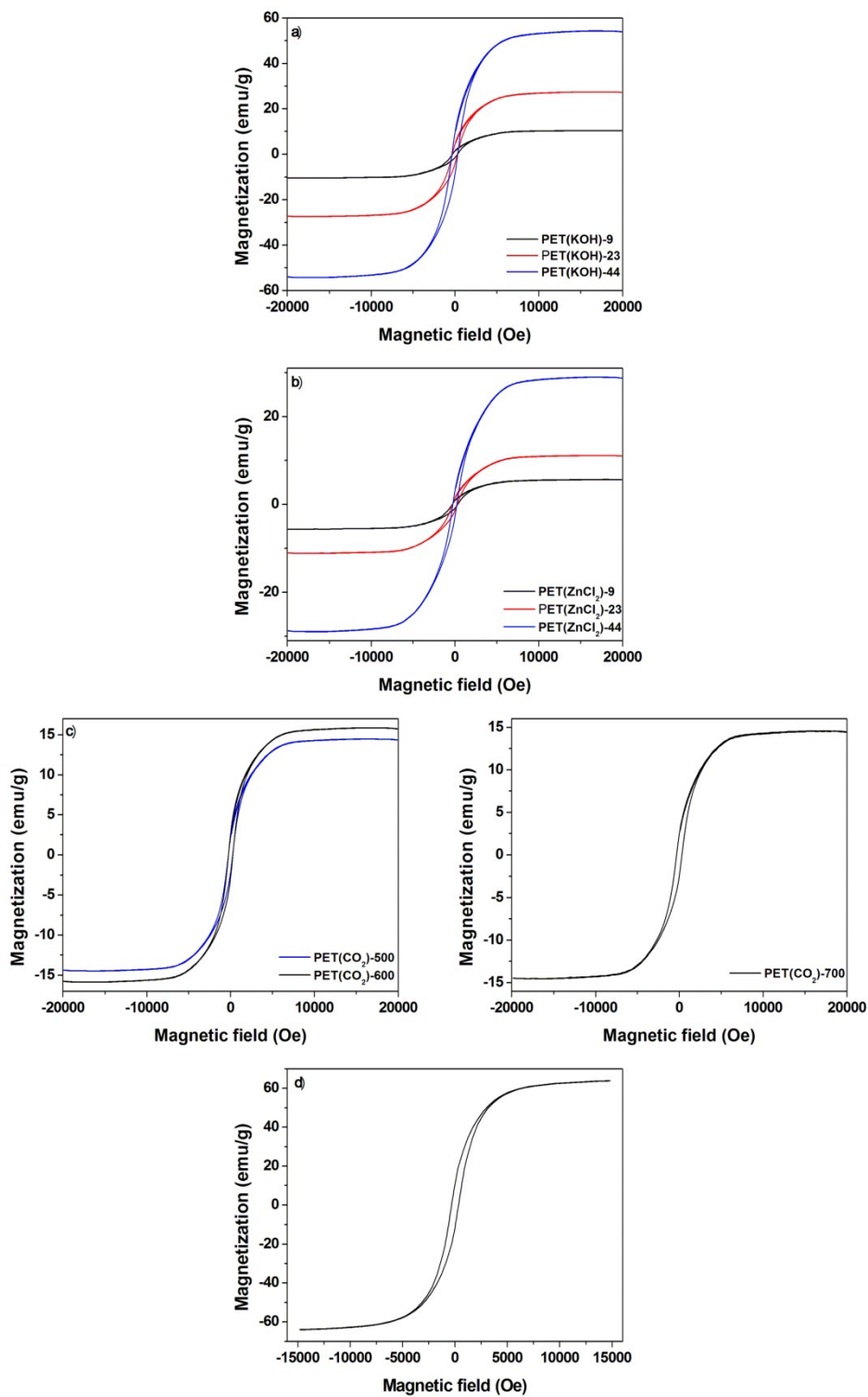


Figure S6. Hysteresis loop of composites activated with (a) KOH, (b) ZnCl<sub>2</sub>, (c) CO<sub>2</sub> and (d) hysteresis loop of pristine carbon encapsulated iron nanoparticles.



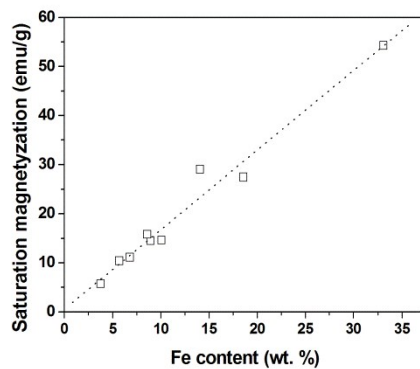


Figure S7. Saturation magnetization vs. Fe content (data for all composites).

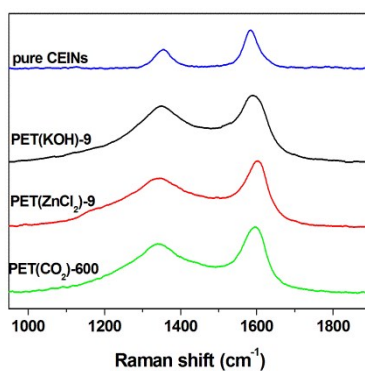


Figure S8. Representative Raman spectra of magnetic composites in comparison to pure CEINs.

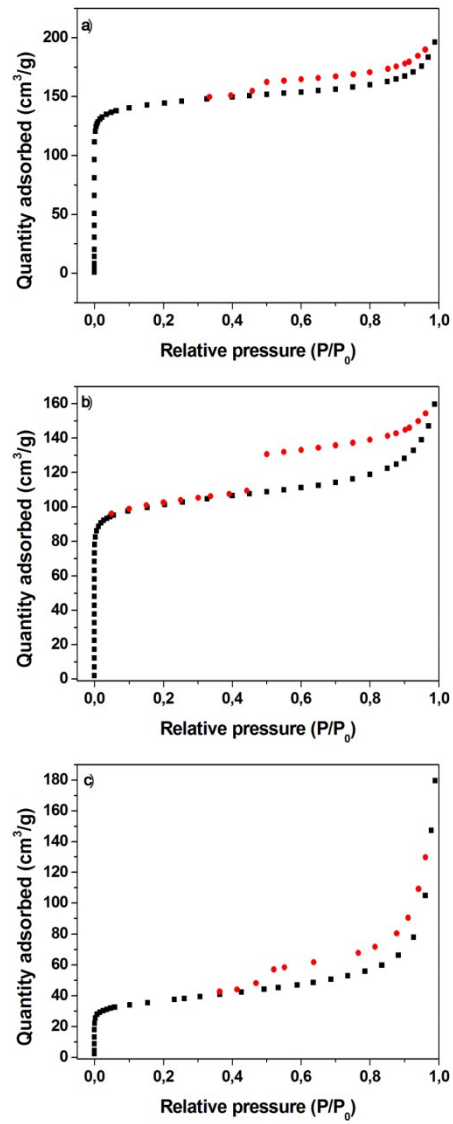


Figure S9. Adsorption/desorption isotherms of N<sub>2</sub> at 77K onto (a) PET(KOH)-9, (b) PET(KOH)-23, (c) PET(KOH)-44.

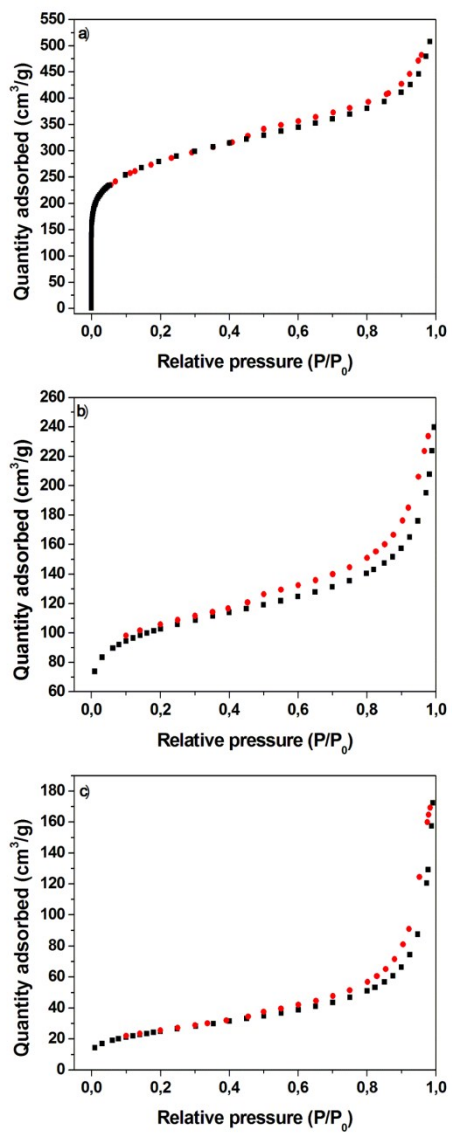


Figure S10. Adsorption/desorption isotherms of N<sub>2</sub> at 77K onto (a) PET(ZnCl<sub>2</sub>)-9, (b) PET(ZnCl<sub>2</sub>)-23, (c) PET(ZnCl<sub>2</sub>)-44.

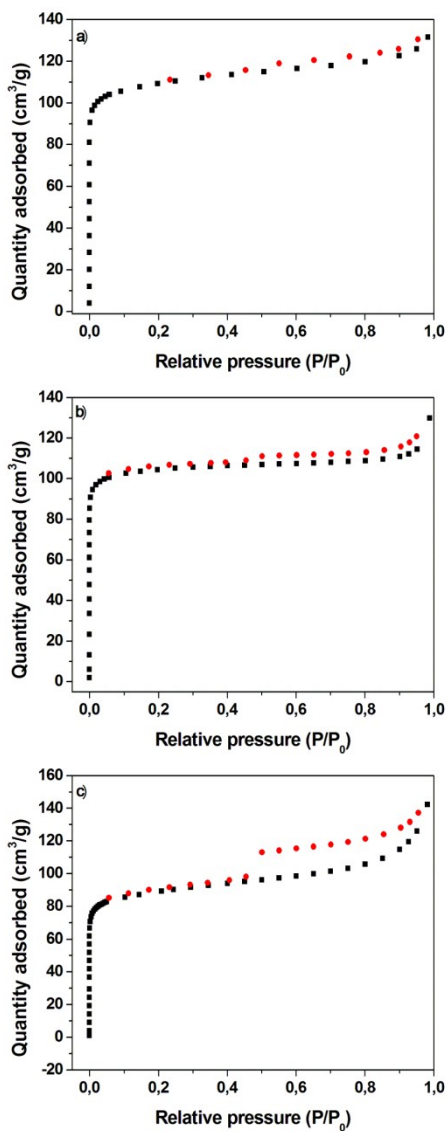


Figure S11. Adsorption/desorption isotherms of N<sub>2</sub> at 77K onto (a) PET(CO<sub>2</sub>)-550, (b) PET(CO<sub>2</sub>)-600, (c) PET(CO<sub>2</sub>)-700.

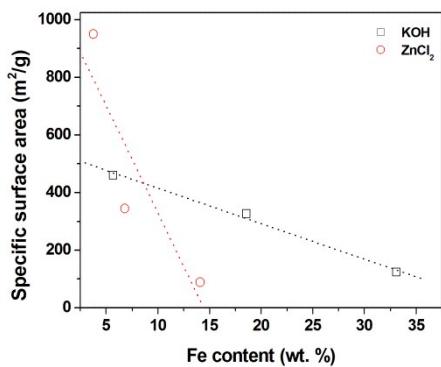


Figure S12. Specific surface area vs. content of Fe for KOH and ZnCl<sub>2</sub> activated composites.

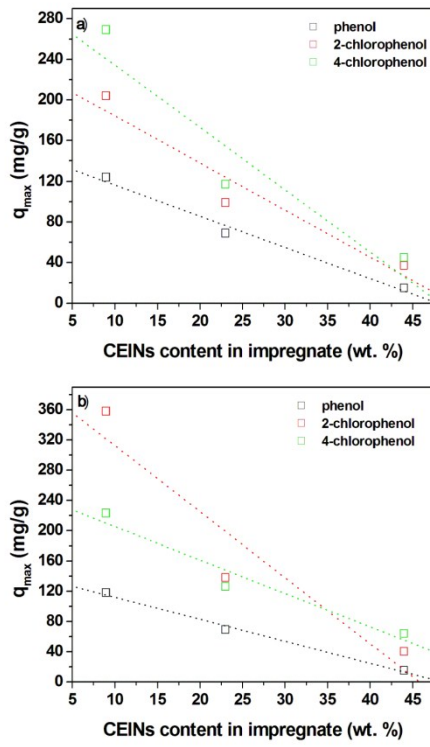


Figure S13. Dependence between evaluated  $q_{max}$  and content of CEINs for (a) PET(KOH) and (b) PET(ZnCl<sub>2</sub>) composites.

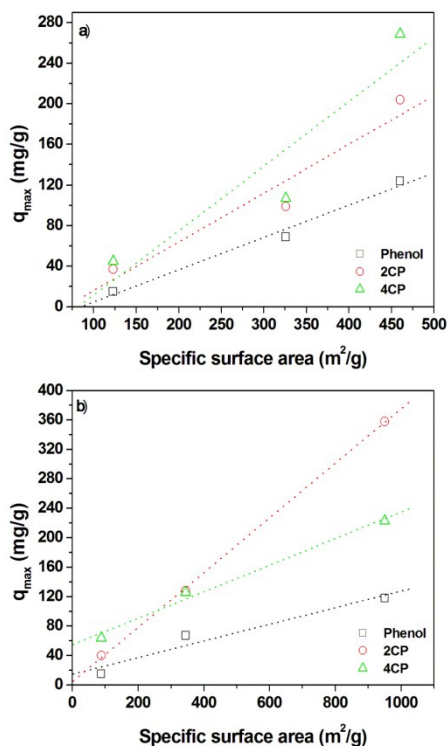


Figure S14. Correlation between evaluated  $q_{max}$  and specific surface area for (a) KOH and (b)  $ZnCl_2$  composites.

### The importance of one-step synthesis method

The above presented data directly indicated that zinc chloride is the best activating. Therefore additional experiments have been conducted to check whether the use of the mixture used for PET dissolution (phenol and 1,1,2,2-tetrachloroethane) is important. Three additional composites have been synthesized, and the content of CEINs was kept constant at 9 wt.%. The composite named 'non-activated' has been synthesized according to the procedure given in experimental, however, without subsequent activation. The composite 'one-step, no solvents' has been obtained with activation, however, the initial materials, i.e. CEINs, PET and  $ZnCl_2$  were mechanically mixed together. Finally, the composite 'two-step, solvents' has been fabricated via the step method. The first step included the carbonization (600°C) of PET, CEINs and solvent mixture. The as-obtained powder was mixed with  $ZnCl_2$  and activated at 700°C. The mass ratio between  $ZnCl_2$  and PET was 3:1. Figure S15 shows the adsorption isotherms of phenol onto the composites produced in different ways. It is evident that adsorbents obtained in the one step method (activating agent directly mixed with PET) have better adsorption performance. This is because the observed uptakes are 2.5-3.3 times higher in comparison to the non-activated material. Interestingly, the non-activated material is characterized by a relatively high adsorption capacity (23 mg/g). The comparison of 'one-step, solvents' and 'one-step, no solvents' brings a conclusion that the solvent of PET (phenol – 1,1,2,2-tetrachlorethane) is a factor which preliminary develops the composite porosity.

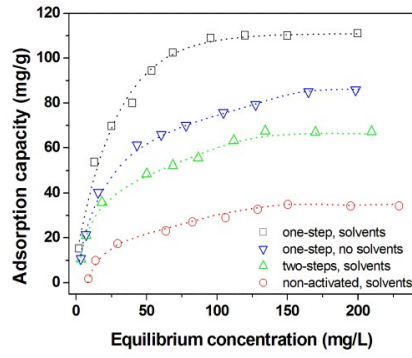


Figure S15. Adsorption isotherm of phenol onto  $ZnCl_2$  activated composites obtained with different methods

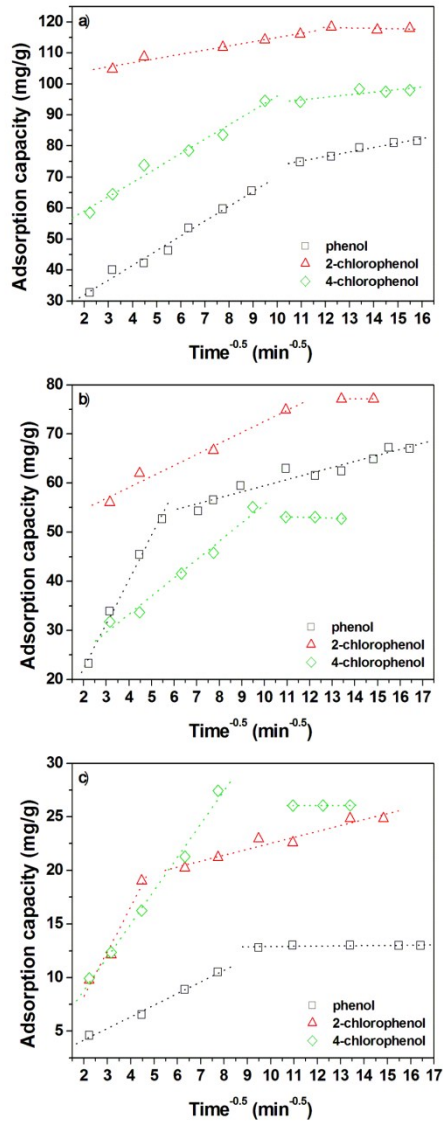


Figure S16. Intra-particle diffusion plots for (a) PET(KOH)-9, (b) PET(KOH)-23 and (c) PET(KOH)-44.

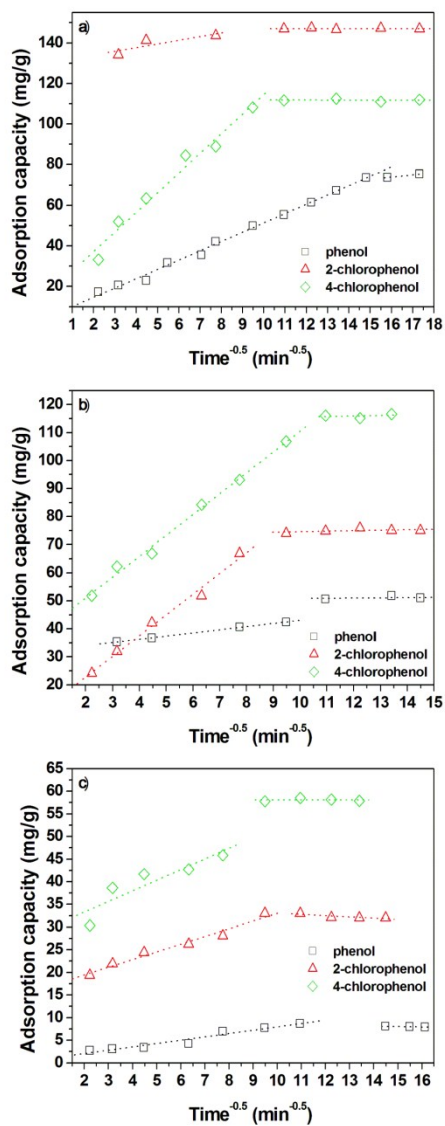


Figure S17. Intra-particle diffusion plots for (a) PET(ZnCl<sub>2</sub>)-9, (b) PET(ZnCl<sub>2</sub>)-23 and (c) PET(ZnCl<sub>2</sub>)-44.



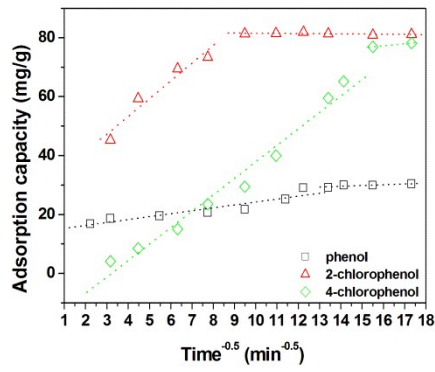


Figure S18. Intra-particle diffusion plots for PET(CO<sub>2</sub>)-600.

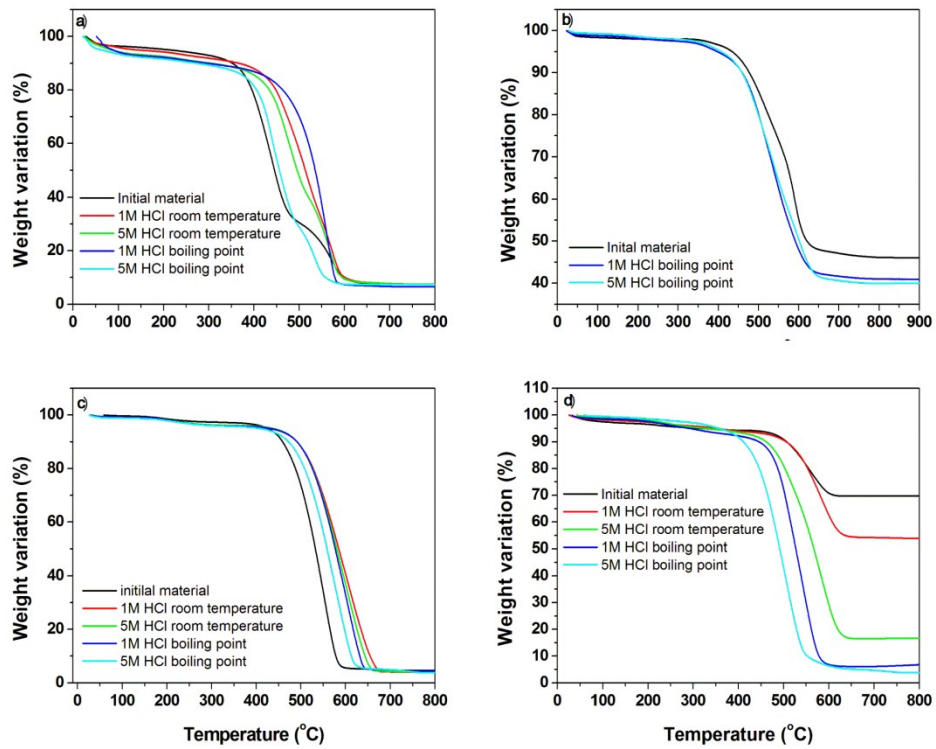


Figure S19. Thermogravimetric curves of (a) PET(KOH)-9, (b) PET(KOH)-44, (c) PET(ZnCl<sub>2</sub>)-9, (d) magnetic composite of activated carbon after corrosion tests.

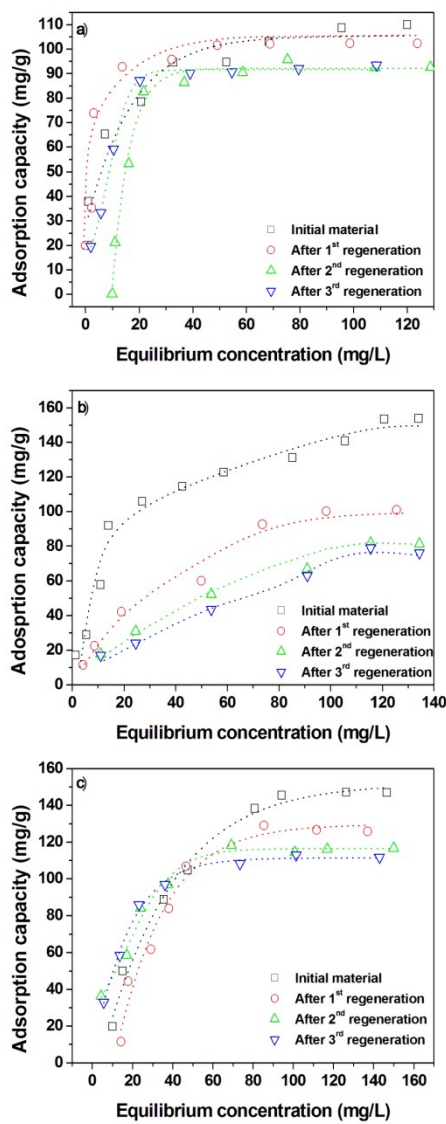


Figure S20. Adsorption isotherms of (a) phenol, (b) 2-chlorophenol, (c) 4-chlorophenol onto PET(KOH)-9 for three adsorption-desorption cycles.

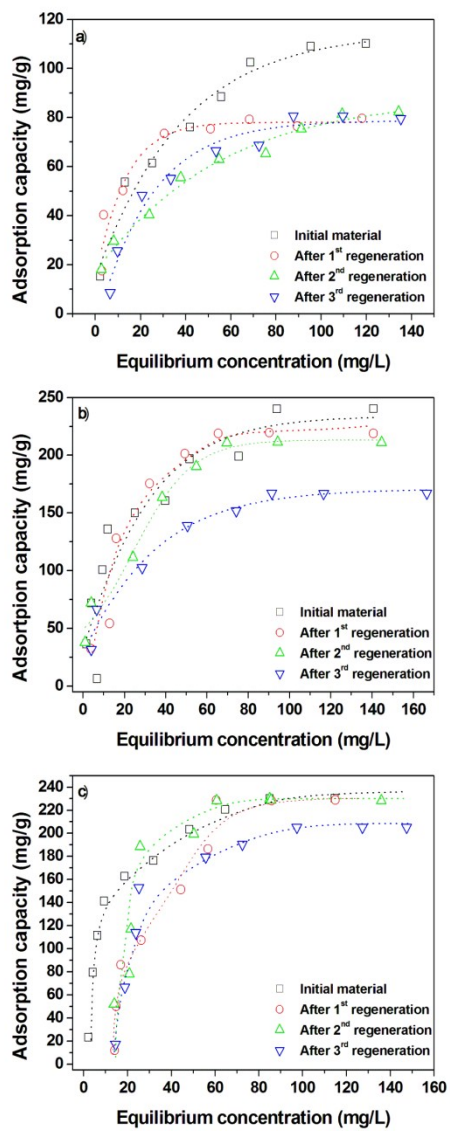


Figure S21. Adsorption isotherms of (a) phenol, (b) 2-chlorophenol, (c) 4-chlorophenol onto PET(ZnCl<sub>2</sub>)-9 for three adsorption-desorption cycles.

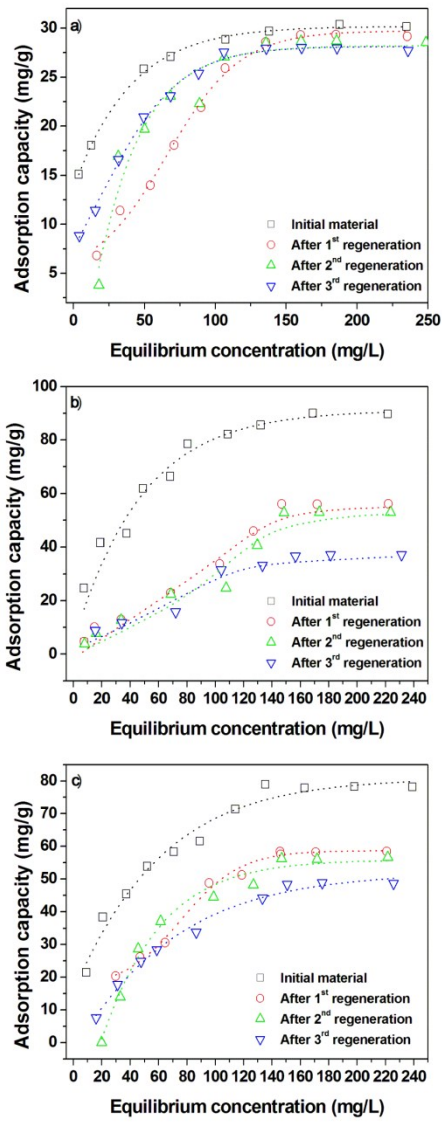


Figure S22. Adsorption isotherms of (a) phenol, (b) 2-chlorophenol, (c) 4-chlorophenol onto PET(CO<sub>2</sub>)-9 for three adsorption-desorption cycles.